



Multi-regional comparison of scarring and pigmentation patterns in Cuvier's beaked whales

Frazer G. Coomber^{1,2} · Erin A. Falcone³ · Erin L. Keene³ · Gustavo Cárdenas-Hinojosa^{4,5} · Rodrigo Huerta-Patiño^{5,6} · Massimiliano Rosso⁷

Received: 31 May 2021 / Accepted: 5 January 2022 / Published online: 22 April 2022
© The Author(s) under exclusive licence to Deutsche Gesellschaft für Säugetierkunde 2022, corrected publication 2022

Abstract

Recent research on Cuvier's beaked whales (*Ziphius cavirostris*) from the Mediterranean has demonstrated that sexes can be visibly distinguished in photos using sex-linked patterns of scarring density and pigmentation, even at age classes which are notoriously difficult to differentiate. Being able to apply this research to other populations would allow for better monitoring of population demographics and vital rates globally. This study uses Photo Identification Captures (PICs) of known sex, adult Cuvier's beaked whales from three regions (Southern California, USA; Guadalupe Island, Mexico; and the Mediterranean Sea, Italy) to evaluate geographic variation in sex-linked patterns of scarring density and pigmentation. Standardized scarring density measurements from typical photo-ID views and Generalized Linear Models (GLM) were used to identify scarring density thresholds for sex at each region and for all regions combined to predict the sex of individuals. Scarring densities did not differ significantly among regions and thresholds calculated from any region correctly predicted the sex in other regions 92–98% of the time. An agglomerative cluster analysis with complete linkage identified three distinct pigmentation clusters in each of the three regions, with one being indicative of sex. This study supports the notion that scarring density is indicative of sex for this species, improves the predictive capacity of this metric inter-regionally, and provides a reliable method to estimate the sex of whales in a typical photo-ID catalog, thus supporting vital rate assessments for this data-deficient species.

Keywords Cuvier's beaked whale · Photo identification · Vital rates · Geographic comparison · Pigmentation patterns

Introduction

The ability to accurately identify the sex and age of individuals within a population is an important aspect of cetacean ecology. The sex and age of a cetacean has been shown to influence social interactions (Weiss et al. 2021), the rate of inter-specific competition (Lee et al. 2019), and individual survival (Civil et al. 2018) and mortality rates (Ijsseldijk et al. 2020). Vital rates, relative changes in the survival and mortality parameters of a population over a set time period, can provide valuable insights into population health, and

Handling editors: Stephen C.Y. Chan and Leszek Karczmarski.

This article is a contribution to the special issue on “Individual Identification and Photographic Techniques in Mammalian Ecological and Behavioural Research – Part 1: Methods and Concepts” — Editors: Leszek Karczmarski, Stephen C.Y. Chan, Daniel I. Rubenstein, Scott Y.S. Chui and Elissa Z. Cameron

✉ Erin A. Falcone
efalcone@marecotel.org

¹ Mammal Society, Black Horse Cottage, 33 Milton Abbas, Blandford Forum, Dorset DT11 0BL, UK

² The University of Sussex, Sussex House, Falmer, Brighton BN1 9RH, UK

³ Marine Ecology and Telemetry Research, Seabeck, WA, USA

⁴ Comisión Nacional de Áreas Naturales Protegidas, Ensenada, Baja California, Mexico

⁵ Proyecto de Investigación Zifido de Cuvier y Otros Cetáceos de Isla Guadalupe, Ensenada, Baja California, Mexico

⁶ Centro de Investigación Científica y de Educación Superior de Ensenada, Ensenada, Baja California, Mexico

⁷ CIMA Research Foundation, Via Magliotto 2, 17100 Savona, Italy

may reveal sub-lethal impacts of anthropogenic stressors before they result in a detectable population decline. They can be particularly useful when the onset or severity of effects may vary by age, sex, or reproductive status, and might be masked if these classes cannot be considered separately with available data (Booth et al. 2020). It has become commonly accepted that the use of mid-frequency active sonar (MFAS) poses a particularly high risk to deep diving species, especially beaked whales (Cox et al. 2006; Hooker et al. 2009). Vital rates are critical elements of energetic and Population Consequences of Disturbance (PCoD) models being developed for beaked whale species to estimate the long-term impacts of MFAS exposure on individuals and the populations they comprise (New et al. 2013; Pirodda et al. 2018). But despite this, many basic life history traits for these species remain poorly documented. Parameters including female calving interval, weaning age, age at sexual maturity, and reproductive lifespan are virtually unknown (MacLeod and D'Amico 2006; Baird 2019). These estimates of population parameters are typically identified through the use of long-term individual-based photographic identification studies (Clutton-Brock and Sheldon 2010; Karczmarski et al. 2022). However, the age and sex of individuals needs to be accurately determined and the sample representative of the population (Perrin and Reilly 1984).

There are multiple ways that cetaceans in the wild can be sexed, including behavioral associations (such as between a female and a calf, e.g., Rosso et al. 2011), direct observation of the genital region (e.g., Knowlton et al. 1994), and more recently through the genetic analysis of tissue biopsies (e.g., Shaw et al. 2003). Moreover, some cetacean species are dimorphic, displaying sexual differences in size (Caspar and Begall 2022), color, head/melon shape and the presence or absence of specific ornaments, e.g., erupted teeth (Mesnick and Ralls 2018). Therefore, many species can also be classified to sex using these distinctive differences. The Cuvier's beaked whale (*Ziphius cavirostris*) is one such species where adult males at the onset of sexual maturity develop erupted teeth (Heyning 1989), a trait that can be used to reliably sex an adult male at sea. However, Cuvier's beaked whales are notoriously difficult to study because they predominantly occur far from shore in small groups and can be difficult to detect during the very limited time they spend at the surface (Tyack et al. 2006; Barlow et al. 2006; Schorr et al. 2014). This makes sexing free-ranging Cuvier's beaked whales even more difficult, whether from biopsies (limited sampling opportunities), identification of erupted teeth (an individual's head may not be visible above the surface), or behavioral observations (only a subset of adult females are associated with a calf at any given time). Consequently, it is likely that many photographic catalogs of this species lack the essential classification of sex and age for a proportion of individuals. On the other hand, if photographed whales

can be accurately classified to age and sex by appearance alone, these photographic data can form the basis of vital rates studies.

Sex specific differences in body scarring level and pigmentation patterns have been reported for a number of cetacean species (e.g., Martin and Da Silva 2006; Orbach et al. 2015; Lee et al. 2019) and have previously been used to determine the sex of wild animals from photographs (e.g., Rowe and Dawson 2009; Brown et al. 2016; Coomber et al. 2016a). Adult Cuvier's beaked whale males are quoted as being more heavily scarred than females (Heyning 1989) and a study conducted in the Mediterranean Sea was the first to quantifiably assess this statement using Generalized Linear Models (Coomber et al. 2016a). In doing so, it presented scarring density thresholds, values relating to the measured density of scarred to unscarred pixels from a photographic identification image, that could be used to reliably differentiate adult male (above threshold) and adult female (below threshold) animals (Coomber et al. 2016a). Inferences relating to sex-linked pigmentation patterns were also analyzed. However, this study was conducted on a limited sample size that used only high-quality, full-body photographic recaptures from a genetically distinct population (Dalebout et al. 2005). The current study, therefore, aims to expand this work by exploring if these methods are applicable across different geographic populations and if there are any geographical variations in these external characteristics, and also to develop the methods that can be applied more broadly to typical photographic identification images that do not include full-body sequences. To achieve this, the pigmentation classification and scarring density methods used previously will be applied to whales from two distant populations of Cuvier's beaked whales in the Pacific Ocean, one from Southern California, USA and the other from Guadalupe Island, Mexico. Scarring density threshold modeling and pigmentation cluster classification techniques were applied to a sample of independently sexed adults from each of these three populations, including the whales from the original Mediterranean Sea study, to examine the extent to which these diagnostic traits vary geographically within this widely distributed species, and which can further be applied to sex whales throughout the species range.

Methods

Data collection

A dataset of Photographic Identification Captures (PICs, the photographic documentation of a unique individual on a given date) of Cuvier's beaked whales was sourced from three geographic regions: the vicinity of the Southern California Antisubmarine Warfare Range, a MFAS training

area approximately 140 km off the coast of Southern California, USA (CAL), the oceanic Guadalupe Island located 260 km west of Baja California in the Mexican Pacific Ocean (GUAD), and the Ligurian Sea in the North-West Mediterranean Sea (MED) (Rosso et al. 2011; Coomber et al. 2016a; Fig. 1). In each study, groups of whales were approached with the goal of photographing each individual as completely as possible from the rostrum to the tailstock, though the minimum requirement for a successful PIC was one high-quality perpendicular view of either side of the dorsal body surface including the dorsal fin (See Appendix, Fig. A1). The CAL population has been the subject of dedicated photo-identification (photo-ID) research since 2006 (Falcone et al. 2009; Curtis et al. 2020). The regional catalog available for this study included 473 PICs of 250 unique individuals through 2019. Individuals in the GUAD population were photographed opportunistically as early as 2006 (Cárdenas-Hinojosa et al. 2015), with dedicated photo-ID research beginning in 2016. The available catalog from GUAD through 2019 included 677 PICs of 82 individuals. Individuals in the MED population were opportunistically photographed beginning in 1998, with dedicated effort since 2004 (e.g., Rosso et al. 2011). The MED catalog through 2019 was composed of 248 individuals documented by 2395

PICs. Given the relative proximity of the study areas, identified individuals from the CAL and GUAD regional catalog were cross-examined to establish if any animal was present in more than one catalog.

From each PIC, a representative series of photos of one side of the body were selected for age classification (via visible diagnostic traits), visible body division, and scarring density measurement generally following the methods described in Rosso et al. (2011) and Coomber et al. (2016a), which used the same MED dataset considered here. Individuals showing erupted teeth were assumed to be adult males (hereafter AM) and toothless whales with paling on the head that surfaced in close association with a calf (a uniformly dark individual less than two-thirds the adult length) were categorized as adult females (hereafter AF), with sexes confirmed genetically when possible. Predominantly dark-bodied animals with little or no pale pigmentation on or near the head and that lacked erupted teeth and were not sighted in association with a calf were presumed to be immature and excluded from the study, along with apparently mature individuals that had no photographic documentation of these same sex-confirming traits.

The subset of analyzed PICs were collected between 2004 and 2019 and included 186 suitable quality PICs from 117

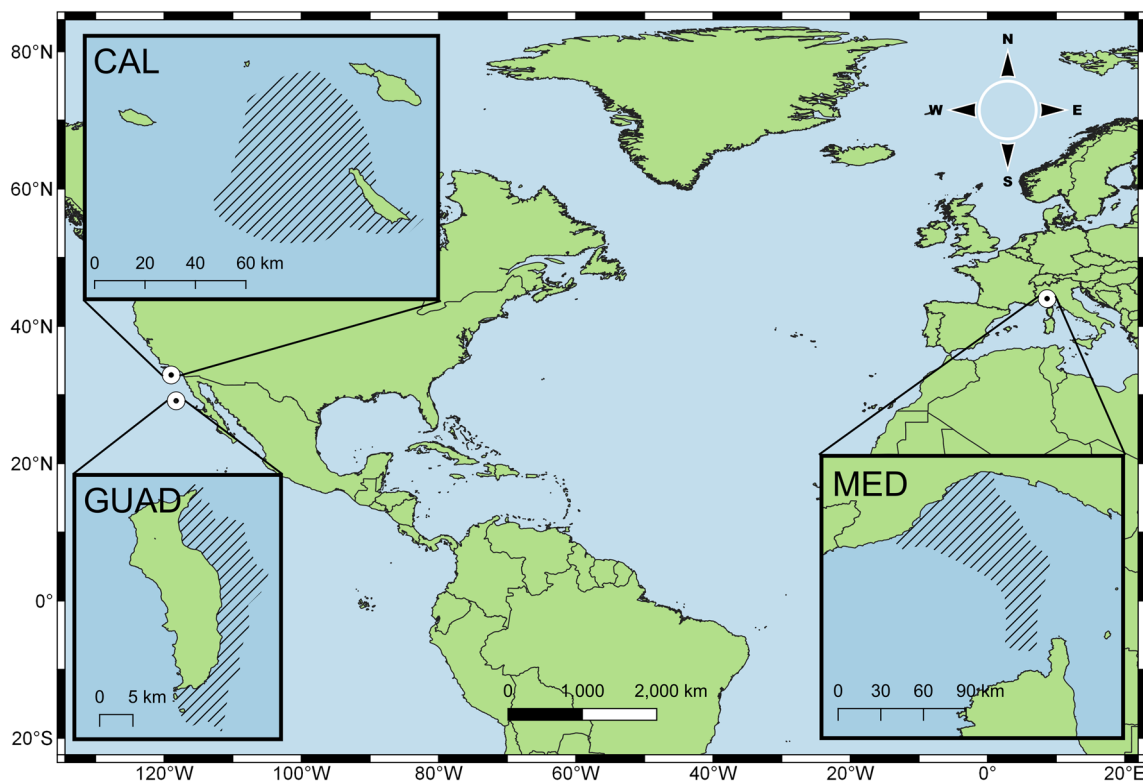


Fig. 1 Global positions of the three geographic regions considered in the present study, with primary data collection areas for Cuvier's beaked whales within each region indicated by hashed areas in inset

maps, including: Southern California, USA (CAL), Guadalupe Island, Mexico (GUAD), and the Mediterranean Sea (MED)

Table 1 The total number of available photographic identification captures (PICS) of known-sex Cuvier's beaked whales by region with information on measured scarring densities

Population	Number of PICS	Number of unique adult males (AM)	Number of unique adult females (AF)
CAL	85	32	20
GUAD	53	11	6
MED	48	26	22

adult individuals of known sex (48 AF and 69 AM; Table 1) from all three regions. The set of representative photos from each PIC were independently quality scored (scale of 1–3 from best to worst), for the following three factors: proportion of the body visible above the water line, image exposure/lighting, and image sharpness/focus.

Delineation of body into regions of interest (ROI)

The previous Mediterranean study (Coomber et al. 2016a) only used PICs that included images from the head to the tail stock in its analysis. These PICs were delineated into Regions of Interest (ROIs) based on the morphometric information that the length from the anterior to posterior insertion points of the dorsal fin is roughly one-seventh the distance from the blowhole to the anterior dorsal fin insertion in this species (Heyning 1989). Using ImageJ version 1.51g (Rasband 2011) and an image from each PIC that included both the blowhole and anterior insertion point of the dorsal fin, the visible body from the blowhole through the dorsal fin could be divided into seven equal sections (ROI₂₋₈). ROI₉₋₁₃ were delineated by extrapolating the width of these sections posteriorly. To expedite the delineation process for the two new catalogues (CAL and GUAD) and to allow the use of PICs that did not contain an image that included both the blowhole and dorsal fin, a Bezier Curve Dividing Macro and an Angle Bisecting Macro (Supplementary Information 1; Eric Keen, Marine Ecology and Telemetry Research) were developed, and the distance from the anterior to posterior dorsal fin insertion points was used to divide the visible surface of the animal into standardized ROIs that were comparable to those in the MED data.

To ensure that data from the different geographic regions were comparable and to maximize the available sample size, the overall frequency distribution of available ROIs was calculated. This was achieved by counting the number of ROIs available from the 186 PICs of known-sex adult Cuvier's beaked whales. This frequency distribution indicated that PICs with data from ROI₇ to ROI₁₀ (the typical minimum photo coverage for a successful PIC; Fig. 2A) were most readily available, but limiting this selection to PICs containing either ROI₇₋₉ or ROI₈₋₁₀ increased the available sample size further (Fig. 2B). However, this dataset included

Table 2 The final number of male and female individuals from each geographic region in the dataset used for the scarring density modeling, after the inclusion criteria were applied

	CAL (<i>n</i> = 36)	GUAD (<i>n</i> = 13)	MED (<i>n</i> = 48)
Adult male (AM)	26 (72%)	7 (54%)	26 (54%)
Adult female (AF)	10 (28%)	6 (46%)	22 (46%)

multiple PICs for the same individual. To ensure that there is no violation of independence within the sample, only one PIC from each individual was considered for subsequent analysis. In these cases, the PIC with the lowest combined quality scores, or the best overall PIC quality, was used. In the case of quality score ties from the same whale, the quality scores were prioritized with proportion visible as first priority and image exposure last. The ROI₇₋₉ was chosen for subsequent analysis as it provided the largest and most balanced dataset with 59 AM and 38 AF after the independence criterion was applied (Table 2). It should also be noted when interpreting results that this dataset is unbalanced with a bias toward AM.

Scarring density threshold analysis

Intraspecific linear scars were identified and traced in ImageJ for each ROI of each individual using the photograph with the largest visible surface area for each available ROI, following the methods of Coomber et al. (2016a). The scarring density, the proportion of scarred to total pixels within a specific ROI or combined ROIs, was calculated by dividing the number of scarred pixels by the total visible pixels within a ROI.

All following analyses were conducted in R Studio version 4.0.3 (R Core Team 2020). To compare the observed mean scarring density between whales of different geographic regions, a one-way analysis of variance (ANOVA) was conducted. If the model assumptions of heterogeneity or normality of variance were violated, identified using a Levene's (Fox 2016) and Shapiro–Wilk's test (Royston 1982), respectively, the non-parametric Kruskal–Wallis equivalent (Hollander et al. 2013) was applied.

To investigate the predictive power of scarring density thresholds between geographic regions, models were fitted to the individual geographic regions and the resultant threshold used to predict the sex of known-sex animals from the other regions. All modeling was conducted within a binomial Generalized Linear Modeling (GLM) framework (Nelder and Wedderburn 1972) or its mixed effect extension (Pinheiro and Bates 2000), with the sex of the animal being the binary response (0 = female and 1 = male) and the scarring density (as the proportion of scarred pixels to unscarred pixels ranging from 0 to 1) within ROI₇₋₉ as the predictor

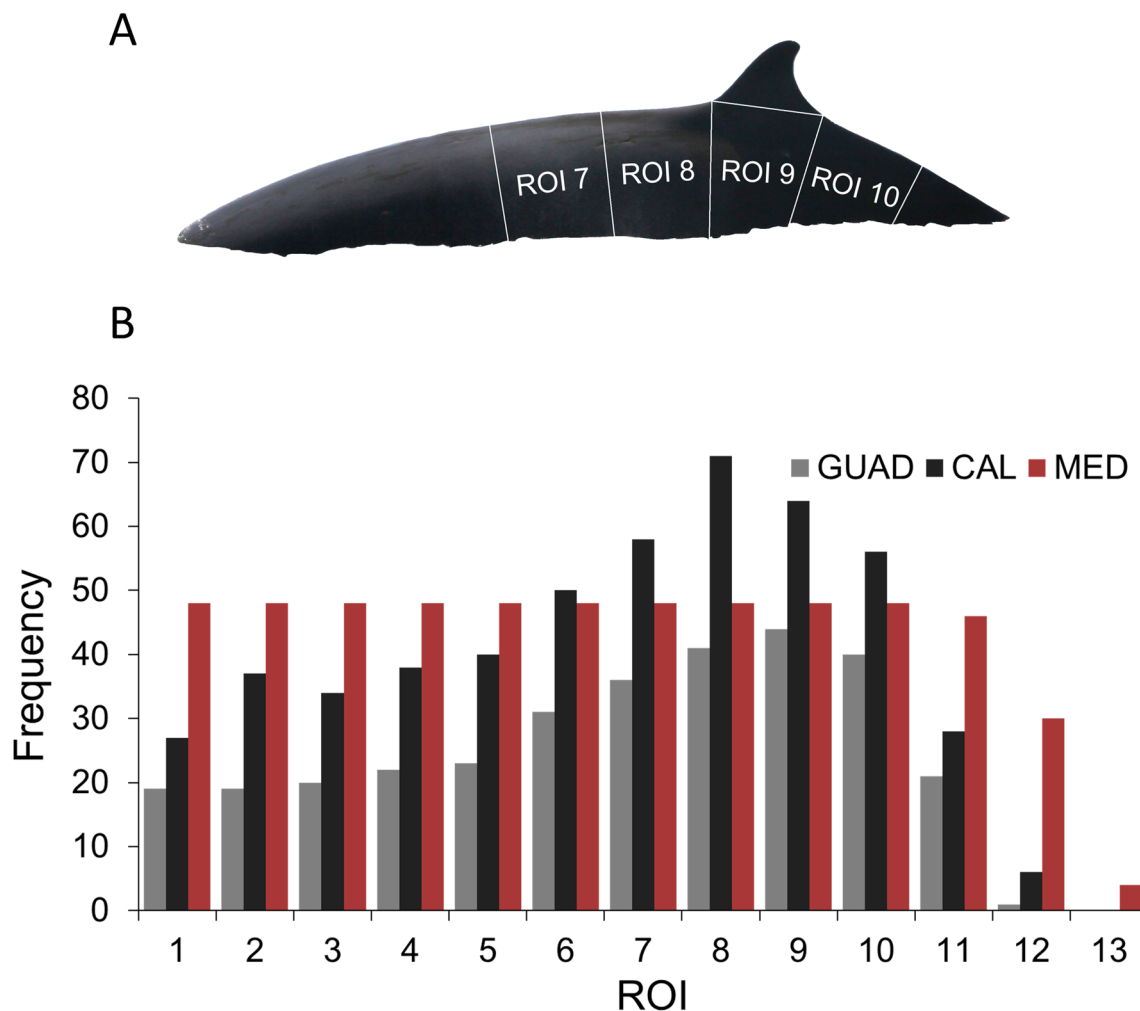


Fig. 2 **A** The typical body view of a Cuvier's beaked whale used for individual identification in most photographic studies, with the four most frequently measured ROIs in this study highlighted. **B** The frequency distribution of scarring density measurements by ROI for

each study region, based on all available PICs. The MED study used only PICs that included the total body surface from ROI₁ through at least ROI₁₀. ROI₇–ROI₁₀ were the most frequently measured ROIs from CAL and GUAD

variable. The original model from Coomber et al. (2016a) was refit, due to recent genetic analysis indicating that one whale's sex was previously incorrectly identified (Baini et al. 2020). To determine the optimum scarring density threshold, Receiver Operating Curve (ROC) methods were used within the R pROC package version 1.17.0.1 (Robin et al. 2011). The threshold value, the scarring density at which individuals with a higher value should be classified as AM, was calculated based on the true positive rate (sensitivity) and true negative rate (specificity) of the MED training data. This threshold was then applied to the testing datasets from GUAD and CAL to predict the sex of adults based on their scarring density relative to the MED threshold at ROI_{7–9}. The discriminatory capability of the model was then measured using the Area Under the (Receiver Operating) Curve (AUC) statistic using the true known sex and threshold predicted sex of each individual. An AUC value of 0.5 indicates

that the model predicts no better than random and a value greater than 0.7 was deemed adequate for good model predictions. This process was then repeated using the data from CAL and GUAD separately as the model training data and the other geographic regions as testing datasets.

Additional candidate models with data from all geographic regions were fitted to further investigate if geographic region influenced the scarring densities and resultant thresholds. The models considered included: a full binomial GLM with no additional regional predictor variables, a binomial GLM with geographic region included as a fixed effect, and a binomial mixed effect GLM that included geographic region as a random effect. If geographic region was included in the best-fit model as a predictor variable, it would indicate that the scarring density threshold results are likely to differ by region and that a threshold from one region may not be applicable to another. To identify which of the candidate

models best fitted the full dataset, model evaluations were conducted using Akaike Information Criterion (AIC; Sakamoto et al. 1986), with the lowest AIC score being considered the best fitting model. Moreover, an ANOVA test was conducted between model residuals to see if the improved fit was statistically significant. The final model, based on the AIC and ANOVA results, was then fitted using combined data from all geographic regions to update the threshold analysis.

Pigmentation data

Each PIC also provided information on external pigmentation features that were shown to be correlated with age and sex in the MED population. These generally followed the patterns defined in Coomber et al. (2016a) and included the presence and appearance of the following features: dark oval patches (“ovals”) on the melon (Appendix Table A1), dark crescents (“crescents”) posterior to the blowhole (Appendix Tables A2, A3), the color of the flanks (i.e., areas of the dorsal surface that were not depigmented, Appendix Table A4), and a depigmented cape extending posteriorly along the dorsal body surface (Tables A5, A6, A7, Fig. A2). However, a more complex set of cape descriptors was used here to better reflect the variability captured in the larger, multi-region sample of sexed adults (i.e., toothed males and reproductive females) in this study. In this case, where an extended cape was present, it was characterized by both its “pattern” (Table A5), i.e., the distribution of depigmented areas along the dorsal surface of the body, and its “texture” (Table A7), i.e., the appearance of those depigmented regions, in addition to its brightness (Table A6) and extent (last ROI to which the cape extends, Fig. A2).

A total of 217 PICs from 148 sexed adults included pigmentation data. However, not all PICs provided information on all pigmentation features; for example, PICs that did not include a good photograph of the head lacked oval data, and in some cases heavy scarring or diatom coverage precluded accurate characterization of the cape. Therefore, PICs were initially filtered to those that included data for the entire set of pigmentation descriptors. In the case where more than one PIC remained for an individual after this filtering, the photo quality criteria applied to the scarring density data

were also applied to the pigmentation dataset to yield a single representative data point for each whale. Following filtering, a total of 120 independent sets of complete pigmentation were available for analysis (Table 3).

Pigmentation analysis

A hierarchical clustering method was applied to the filtered pigmentation dataset to accurately cluster animals with similar pigmentation patterns and differentiate these clusters from each other as much as possible. The first step was to calculate a dissimilarity distance matrix using the daisy function in R (Struyf et al. 1996) with the Gower metric (Gower 1971) in the Cluster package version 2.1.1 (Maechler et al. 2021). The advantage of the daisy function is that it computes dissimilarity matrices using mixed categorical, numeric, and binary data, among others (Struyf et al. 1996).

Two hierarchical clustering approaches were considered, a divisive and an agglomerative clustering method. Divisive represents a bottom-up approach, i.e., start with one big cluster that is subsequently divided based on dissimilarity. Agglomerative clustering—a top-down approach—starts with a number of clusters equal to the number of observations and subsequently groups clusters based on similarity until only one cluster remains (Ackermann et al. 2012). The complete linkage method was used as it finds similar clusters. This method uses the maximum calculated distances between clusters at subsequent stages from the dissimilarity matrix and merges clusters whose maximum distance is minimum (Sharma and Batra 2019). The agglomerative method with complete linkage tends to identify more numerous smaller clusters and was the method chosen for this analysis as it was hoped to provide additional insights to the pigmentation clusters defined in Coomber et al. (2016a). However, the divisive clustering approach, which typically identifies a smaller number of larger clusters, was also considered and the results are provided (Supplementary Information 2). Cluster analyses were conducted in R using the hclust function with a “complete” method for agglomerative and “diana” method for divisive clustering.

To identify the ideal number of clusters for both approaches, the silhouette coefficient was used (Rousseeuw 1986). This coefficient, which ranges from -1 to 1 with 1 indicating good consistency within clusters, was used to measure how close each point in a cluster is compared to the points in the neighboring clusters (Kaufman and Rousseeuw 1990). To test if the distribution of the resultant clusters was dependent on the sex or geographic region, a Chi-squared analysis was used.

Table 3 The number of unique males and females from each region with complete pigmentation data that were included in the pigmentation cluster analysis

	CAL (<i>n</i> =35)	GUAD (<i>n</i> =15)	MED (<i>n</i> =70)
Adult male (AM)	23 (66%)	9 (60%)	41 (59%)
Adult female (AF)	12 (34%)	6 (40%)	29 (41%)

Results

Geographic region scarring density comparison

There were no individuals found in more than one catalog, allowing for a true comparison of scarring density between the independent populations from different geographical regions. Analysis indicated no significant regional differences in scarring density among AM ($\chi^2 = 4.83$, $df = 2$, $p = 0.09$) or AF ($\chi^2 = 2.80$, $df = 2$, $p = 0.25$) at the alpha level of 0.05. Even though the difference cannot be determined statistically due to a limited sample size ($n = 7$), GUAD AM exhibited higher average scarring density ($0.237 \pm \text{SD } 0.065$) than those of AM in MED ($0.170 \pm \text{SD } 0.095$) and CAL ($0.194 \pm \text{SD } 0.075$). AF had very similar scarring densities, but those of CAL AF ($0.014 \pm \text{SD } 0.006$) were slightly lower than those of MED ($0.026 \pm \text{SD } 0.022$) and GUAD ($0.023 \pm \text{SD } 0.011$; Fig. 3). Interestingly, females exhibited much smaller standard deviations when compared to males and there was no overlap between the distribution of scarring density by sex in both CAL and GUAD, whereas there was modest overlap in scarring densities between the sexes in the MED (Fig. 3).

GLM of scarring density thresholds

The GLM fitted to the MED dataset indicated that any animal with a ROI_{7-9} scarring density greater than 0.080 (equivalent to at least 8% of visible pixels within each ROI_{7-9} being scarred) can be classified as an AM with reasonable confidence ($\sim 75\%$ probability, Fig. 4A). Furthermore, this model indicated that animals with a scarring density greater than 0.250 are certainly AM, given the non-existent confidence intervals at this value. Using the 0.080 threshold value

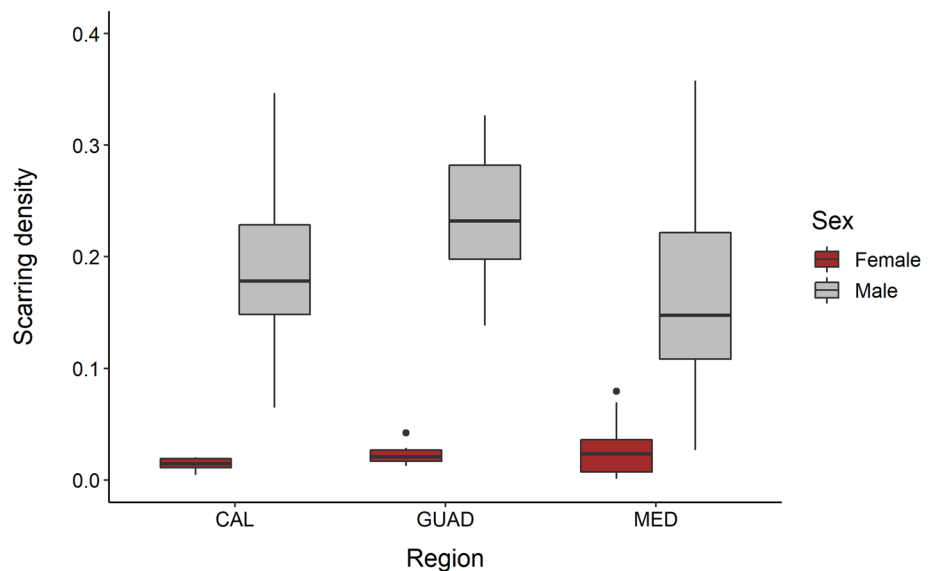
derived from the MED model to classify the sex of independently known sexed CAL and GUAD animals resulted in near perfect predictions of all individuals (98%). The only exception was one CAL AM that was predicted as an AF. The AUC score of 0.985 indicates that the MED model predicts the sex of whales at other geographical regions much better than random.

Similarly, the model fit to the CAL data resulted in a lower scarring density threshold value of 0.043 (Fig. 4B), which correctly predicted the sex of 92% of the MED and GUAD testing animals with an AUC value of 0.913. All GUAD animals were predicted correctly by the CAL model, but one MED AM was classified as an AF and four MED AF as AM. The GUAD data fitted model, with a higher threshold value of 0.090 (Fig. 4C), predicted 92% of animals to the correct sex with an AUC value of 0.933. The animals that were incorrectly identified to sex by the GUAD model were all AM that were classified as AF.

Of the three candidate models considered for the combined scarring density data, the GLM with no regional fixed or random effects was shown to be the best fitting model based on the lowest AIC value (25.75), when compared to the GLMs with either fixed (28.96) or random effects (27.75) for region. Although the AIC scores were close, the difference was at least 2, indicating that adding a random or fixed effect did not improve model fit. Furthermore, the ANOVA Chi-squared test of the residuals indicated that the addition of a fixed effect did not significantly improve a model with no regional covariates ($df = 2$, $p = 0.67$).

Fitting the model to the combined dataset resulted in a scarring density threshold of 0.082 or 8.2% of pixels scarred that predicted the correct sex of nearly all animals (95%), incorrectly predicting five AM sexes as AF with an AUC score of 0.958 (Fig. 5). The inclusion of a larger dataset also

Fig. 3 Boxplots of the observed scarring densities for adult males and females by region



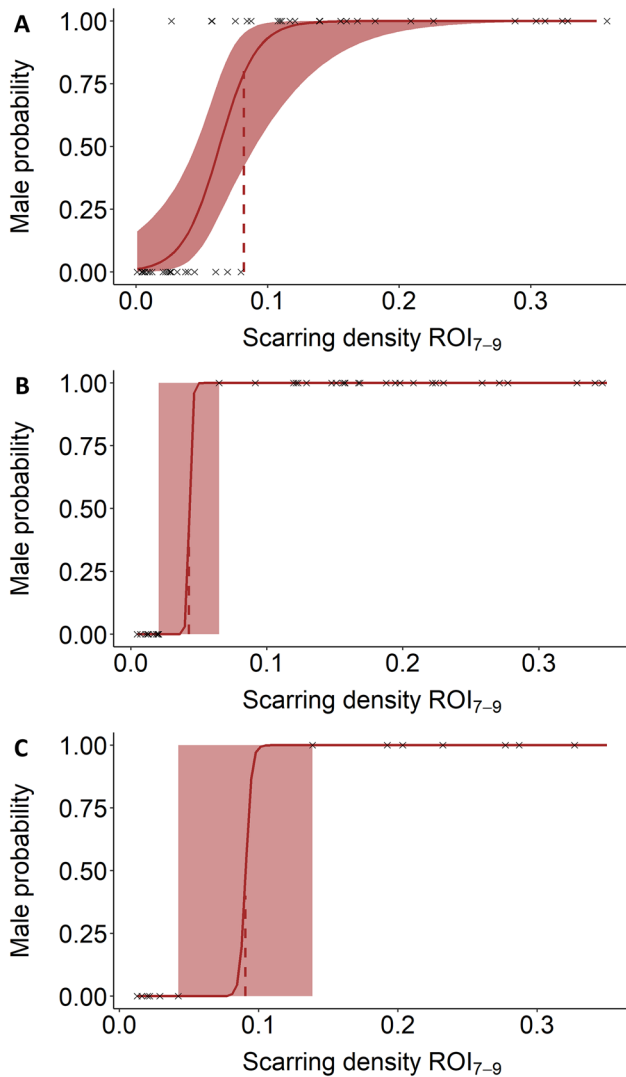


Fig. 4 The GLM fitted to each of the three regional datasets, with the regional scarring density threshold cut-off for males from **A**—MED (0.080); **B**—CAL (0.043); and **C**—GUAD (0.090) indicated by dashed lines. Shaded regions represent the confidence intervals for the MED model and the region between the highest female and lowest male scarring densities for the CAL and GUAD models. These thresholds are based on data from the dorsal fin zone (DFZ) of the body, in this case ROI₇₋₉. Cross marks represent the observed scarring densities for adult males (top) and adult females (bottom) in the filtered data from each region (Table 2)

decreased the confidence intervals for the model (Fig. 5), such that any animal with a scarring density of at least 0.200 is certainly an AM, regardless of region.

Pigmentation patterns

The agglomerative hierarchical clustering approach and the silhouette method, with a coefficient of 0.425, suggested that there were three distinct pigmentation clusters (Figs. 6, 7). The number of individuals and sexes for the three clusters

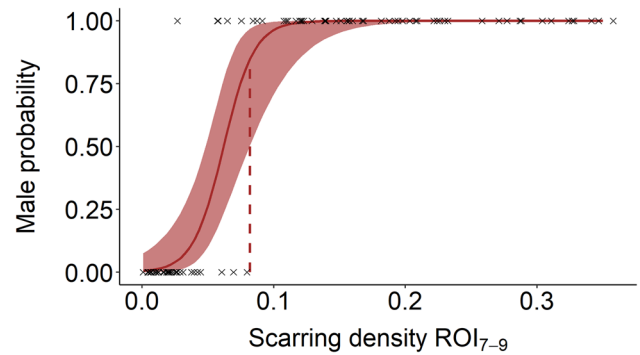


Fig. 5 The best-fit model (binomial GLM with no fixed or random effects) of scarring density for males based on combined data from all regions, with the male scarring density threshold (0.082, dashed line) and the confidence intervals (shaded region) indicated. These thresholds are based on data from the dorsal fin zone (DFZ) of the body, in this case ROI₇₋₉. Cross marks represent the observed scarring densities for adult males (59 individuals, top) and adult females (38 individuals, bottom) in the filtered data

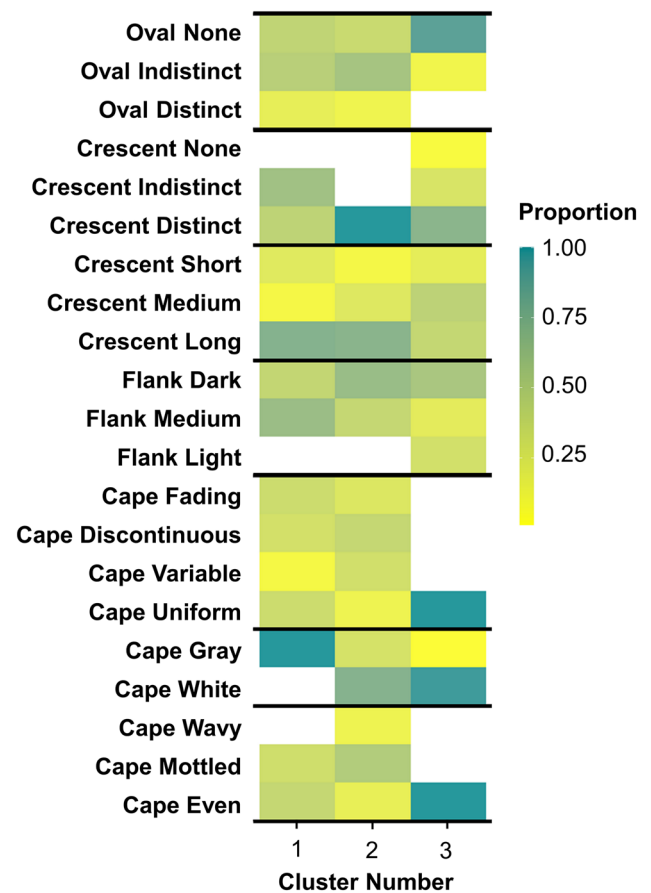


Fig. 6 The results of agglomerative hierarchical clustering based on pigmentation features. Darker shades indicate a higher proportion of individuals in the cluster with a given appearance for each pigmentation feature considered

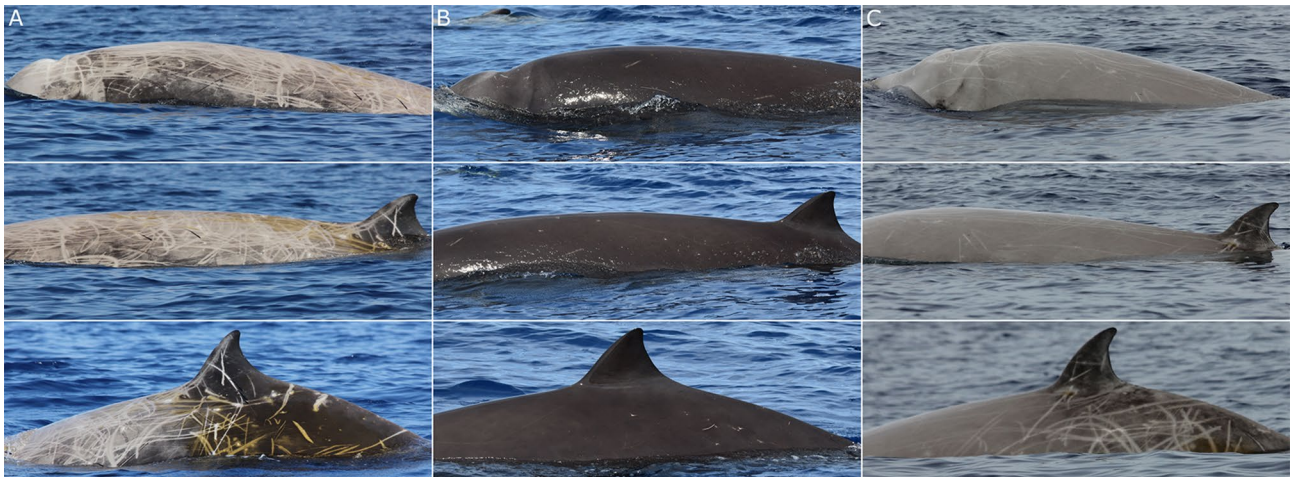


Fig. 7 Examples of individuals in the three pigmentation clusters identified in the current study: **A** an adult male in Cluster 1, **B** an adult female in Cluster 2, and **C** an adult male in Cluster 3

Table 4 The frequency distribution, including the percent of the animals within each cluster, by sex

	Adult male (AM)	Adult female (AF)
Cluster 1 ($n=35$)	23 (66%)	12 (34%)
Cluster 2 ($n=22$)	0 (0%)	22 (100%)
Cluster 3 ($n=65$)	50 (79%)	15 (21%)

Table 5 The frequency distribution, including the regional percent of the animals within each cluster, for each geographic region

	CAL ($n=35$)	GUAD ($n=15$)	MED ($n=70$)
Cluster 1	13 (37%)	8 (53%)	14 (20%)
Cluster 2	5 (14%)	4 (27%)	13 (19%)
Cluster 3	17 (49%)	3 (20%)	43 (61%)

are summarized in Table 4. Cluster 1 included a high percentage of animals with ovals of varying appearance, distinctive long crescents, variable or discontinuous gray or white capes, and a medium or dark flank color. Cluster 2 had animals that had predominantly indistinct ovals and indistinct long crescents, a fading gray cape, and a medium flank color. Cluster 3 included animals that typically lacked ovals, had distinct long crescents, a white even cape of uniform texture and dark flank coloration.

The distribution of the sexes between the clusters was significantly different to an even distribution ($\chi^2 = 43.60$, $df=2$, $p < 0.01$) with Clusters 1 and 3 having predominantly AM at 66% and 79%, respectively, and Cluster 2 being all AF (Table 4). All clusters were represented within each geographic region (Table 5), although the frequencies

were shown to differ significantly from an even distribution ($\chi^2 = 10.85$, $df=4$, $p=0.03$). However, the approximation of the test statistic may be subject to potential biases from the low expected values, especially for the GUAD animals. Furthermore, comparing the distribution of animals within clusters between just CAL and MED, with their larger sample sizes, the distribution of animals within clusters was not significantly different ($\chi^2 = 3.59$, $df=2$, $p=0.17$).

Within the available dataset, there were 47 animals (29 AM and 18 AF) that had scarring densities for ROI₇₋₉ and that were classified into a pigmentation cluster. When comparing the scarring densities of AM in Clusters 1 and 3 (Cluster 2 was not considered as it contained only AF), there was no significant difference ($F=0.28$, $df=1$, $p=0.60$). In fact, the average scarring density for Cluster 1 AM ($0.198 \pm \text{SD } 0.072$) was very similar to that of Cluster 3 AM ($0.170 \pm \text{SD } 0.093$), with both clusters having average scarring densities very close to the male certainty cut-off threshold of 0.2. In the case of AF, the scarring density was also not found to be significant among clusters ($F=2.49$, $df=1$, $p=0.13$), with average scarring density within Cluster 1 ($0.034 \pm \text{SD } 0.032$), Cluster 2 ($0.024 \pm \text{SD } 0.013$), and Cluster 3 ($0.014 \pm \text{SD } 0.017$) being similar. However, great care should be taken when interpreting these results due to the low number of animals analyzed.

Discussion

A previous study of Cuvier's beaked whales from the Mediterranean Sea found that scarring density thresholds from complete photographic sequences of the entire body surface can be used to reliably sex known adult animals from the same population (Coomber et al. 2016a). This study has

continued this work and confirmed that this method can also successfully be applied to at least two geographically distant Cuvier's beaked whale populations off the coast of California (USA) and at Guadalupe Island (Mexico). The findings that sex-based scarring densities do not differ significantly among these three geographic regions, that models fitted to distinct geographic regions can correctly predict the sex of nearly all known-sex adults from other regions, and that including geographic region as a covariate in a full model does not improve its fit all support this statement. Therefore, these findings suggest the plausibility of combining data across regions into a single model, which, when applied in this study, improved the model's predictive accuracy through the narrowing of confidence intervals.

The original Coomber et al. (2016a) study identified just two pigmentation clusters among known-sex adults in the Mediterranean sample: the pigmentation features in these "soft" and "sharp" clusters were comparable to Clusters 2 and 3, respectively, in the present work. The addition of more detailed pigmentation descriptors and additional individuals in the current study identified a third cluster. This new cluster, which is best described as whales with extended capes that are variable in color, pattern, and texture, included both males and females like the previously defined "sharp" pigmentation cluster. However, the uniquely adult female "soft" cluster (Coomber et al. 2016a) remained distinct in this larger, multi-regional sample of known-sex adults.

While all three clusters are present in all three regions, it remains true that only Cluster 2, the equivalent of the "soft" cluster, is diagnostic of sex in adults. This suggests that while pigmentation differentiation is a common trait in adults throughout the species range, only a limited number of adults (females in Cluster 2) can be reliably sexed by their pigmentation pattern alone. It should also be noted that a combination model, which included both pigmentation pattern and scarring density as predictors of sex, was considered for these data but failed to converge, due in part to the limited sample size of whales that had both complete pigmentation pattern classifications and scarring density metrics at ROI₇₋₉. Coomber et al. (2016a) successfully combined pigmentation and scarring density metrics in a common model based on full photographic sequences, but pigmentation characteristics were not retained during model selection, potentially due to the much higher predictive power of scarring density. Thus, while pigmentation differentiation remains necessary to confirm the onset of sexual maturity (Rosso et al. 2011), scarring density remains the more broadly applicable method of sexing adult whales (Coomber et al. 2016a).

In addition to developing several tools that greatly expedite the procedures required to consistently derive scarring density measurements (Supplementary

Information 1), another important finding of this study was that complete photographic sequences were not required to correctly predict the sex of adult whales. We modeled sex-based scarring density thresholds using only the areas of the body just anterior to and below the dorsal fin. This is the typical view of the body that is used in photo-ID studies of this species and, thus, readily available for most whales in any study population. Given that it can be difficult to completely photograph individuals of this species in many circumstances, photos documenting tooth eruption and close calf association, and complete sequences from the rostrum to the tail are often lacking for many individuals in photo-ID catalogs. Indeed, the bias towards males in this study may be because all adult males have erupted teeth while only some adult females will have an attendant calf at any given time, limiting the opportunities to confirm their sex by this standard. It is also important to note that despite all efforts made to not violate the assumption of independence, there is a very small probability that a few animals within the dataset that do not have both a left- and right-side identification photograph may represent replicated samples.

Through the combined use of pigmentation differentiation cues associated with the onset of sexual maturity (Rosso et al. 2011) and the improved methods of deriving scarring density measurements presented here, many, if not most, Cuvier's beaked whales in a typical photo-ID catalog can now be efficiently sexed, with quantifiable confidence levels, using a single, good-quality identification image. The ability to reliably sex individuals in a population has important applications when looking at consequences of disturbance (Booth et al. 2020). Several studies have suggested that the effects of chronic disturbance on beaked whales are likely to be most evident in the female calving interval before they lead to reduced adult survival (Wright et al. 2007; New et al. 2013). While few, if any, ongoing Cuvier's beaked whale photo-ID studies can measure calving intervals directly for even a limited number of females (e.g., by documenting the same female in enough consecutive years to verify the births of all subsequent calves), this rate can be estimated through operational ratios of adult females to calves over shorter (e.g., annual) sampling intervals (Claridge 2013). Therefore, the ability to classify a greater number of adult females more confidently within catalogs, particularly those lacking other sexing characteristics (i.e., genetic confirmation or close association of a calf), will greatly improve operational ratio estimates.

It is worth noting that differentiating between adult females and sub-adult, or young adult, males is likely to remain challenging. These findings continue to suggest that female scarring densities are relatively low compared to mature adult males, especially in CAL and GUAD, and

males may exceed scarring density thresholds quite early in the maturation process; there are confirmed males in both the CAL and MED studies that exceeded them well before their teeth erupted, the cue used to confirm male sex in this sample (Rosso et al. 2011). In theory, rapid scar accumulation may inherently limit the number of younger males that can be confused with adult females in a population at a given time via this method, though further research is warranted. Although no gain rate analyses were conducted here, multiple sets of scarring density measurements exist for many of the whales included in this study, some over extended periods, and as has been done with other species (e.g., Mariani et al. 2016), these repeat measurements could form the basis of a scarring density gain rate analysis in the future. These gain rates could provide an additional data point to separate younger males from females, as scarring gain rates are higher in males than females of the same age for this species (Rosso et al. 2011). This difference in gain rate may explain why the standard deviation of scarring densities is much lower in adult females when compared to males as the variation in density between older and younger females is going to be less pronounced. An approach like this would be particularly relevant for known-sex adults that were also photographed as subadults.

Geographic variation in pigmentation patterns has been reported for other broadly distributed cetacean species, including spinner dolphins (*Stenella longirostris*; Perrin 1972), humpback whales (*Megaptera novaeangliae*; Rosenbaum et al. 1995), killer whales (*Orcinus orca*; Baird and Stacey 1988), and Indo-Pacific humpback dolphins (*Sousa chinensis*; Chen et al. 2018). In contrast, we found that while pigmentation patterns can be quite variable among individuals within a region, the same pigmentation clusters were present in all three distant populations of Cuvier's beaked whales. While the prevalence of these clusters may vary regionally, low sample sizes and expected values preclude accurate testing of the significance of these differences.

When generalizing these results to other populations, it must be remembered that comparisons were only made between three populations, and that only presumed intra-specific scarring was considered. The populations considered here differ dramatically in their spatial, ecological, and anthropogenic regimes. Despite falling within the boundaries of the Pelagos Sanctuary Marine Protected Area (Notarbartolo di Sciara et al. 2008), the range of the genetically distinct MED population (Dalebout et al. 2005) includes areas of high shipping traffic (Coomber et al. 2016b) and contains a number of individuals contaminated by persistent organic pollutants at levels associated with physiological effects in other marine mammals

(Baini et al. 2020). Individuals in the CAL population inhabit an active military training area (Falcone et al. 2009; Curtis et al. 2020), where they are frequently exposed to MFAS and a range of other sound-generating activities known to disrupt foraging (Falcone et al. 2017). In contrast, the GUAD population inhabits a relatively undisturbed national Biosphere Reserve within Mexico (Cárdenas Hinojosa et al. 2015). Ocean-basin gene flow is low for this species (Dalebout et al. 2005), and while the CAL and GUAD populations are geographically much closer to each other than to the MED, there was no documented exchange of individuals between these two catalogs during this study. Given these ecological differences, the similarities in appearance among these three populations suggest it could be fair to assume that the scarring density model presented here is likely to reliably sex adults from other regions. However, it should be tested against a set of independently sexed individuals from any new study area before it is applied to an entire catalog. Further, incorporating other mark types, both naturally occurring (e.g., cookie-cutter shark scars) (Moore et al. 2003; McSweeney et al. 2007; Best and Photopoulou 2016) and anthropogenic in nature (e.g., entanglements and vessel collisions), into a future scarring analysis could provide additional insights into geographic variation in age-linked appearance traits for this species. For instance, anthropogenic scarring rates may reflect processes affecting population vital rates (Feyrer et al. 2021; Wickman et al. 2021).

In conclusion, this study has continued and improved upon previous work looking at the use of identification photographs of Cuvier's beaked whales to infer age and sex of individuals in long-term studies, a basic but necessary element for many ongoing conservation efforts. The main findings provide support that adult sex-specific patterns of pigmentation and scarring are highly similar between whales from very different geographic regions and as such can be used in combination to improve classification thresholds. These combined datasets, and the methods they have validated, offer the potential for more complex analyses in the future by increasing the quantity and resolution of age- and sex-specific life history data for this data-deficient species.

Appendix: Cuvier's beaked whale pigmentation features

The following figures and tables provide detailed descriptions and examples of the pigmentation features applied to whales in the present study.




Fig. A1 The dorsal flanks of two adult Cuvier’s beaked whales off Southern California. This is the typical view used for individual identification in this species



Ovals

See Table A1.




Table A1 Ovals are patches of darker pigmentation on either side of a paler melon. They may vary in presence, contrast, and definition. Ovals can be difficult to accurately characterize without a high-quality photo of the melon. Ovals typically become less defined with age and can be lost completely or maintained well into adulthood

Example	Category	Description
	None	Immature whales lack ovals because they have not begun the depigmentation process. Mature animals may lack ovals because the melon has become uniformly pale.
	Indistinct	Darker pigmentation gently fades into the lighter color of the melon. There is no clearly defined boundary and limited contrast between the pigmented and depigmented areas.
	Distinct	High contrast and clear distinction between the light and dark areas of the melon.

Crescents

See Table A2.




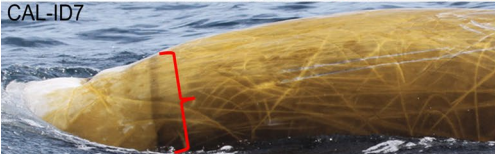
Table A2 Crescents are bands of flank-color pigmentation posterior to the blowhole that are retained during the depigmentation process. They vary in contrast, length, number, and thickness among individuals, and within an individual as it matures. In general, crescents will start out indistinct and become more distinct with time; however, they may shorten over time and no longer be visible above the waterline in mature animals with a very pale cape

Example	Category	Description
	None	Young animals that have not begun the depigmentation process will be uniformly dark and lack crescents. Crescents may also be secondarily reduced in older, very pale animals.
	Indistinct	Low contrast crescents are common in younger animals with limited pigmentation differentiation. They may initially be indicated by regions of paling cape around them.
	Distinct	High contrast crescents are clearly visible against a pale cape.

Crescent length

See Table A3.

Table A3 Crescent length describes how far the crescent extends from the flank to the top of the back. Crescent length changes as an animal ages and crescents may fade gradually along their visible extent. As a result, only the most distinct part of the longest crescent is scored




Example	Category	Description
 CAL-ID149	None	Immature whales without crescents have no crescent length score.
 CAL-ID77	Short	Most distinct segment of crescent extends less than half the distance from the eye to the blowhole and may not be visible at all if whale is low in water. Can be "Distinct" or "Indistinct" and may fade to the top of the back.
 CAL-ID92	Medium	Crescents extend at least half the distance from the eye to the blowhole and are visible above waterline in typical surfacing. Can be "Distinct" or "Indistinct" and may fade to the top of the back.
 CAL-ID7	Long	Crescents extend to or near the topline of the back behind the blowhole and are clearly visible throughout their extent.

Flank color

See Table A4.

Table A4 Flank color is the primary body color outside of the depigmented cape and scarring. In whales with extensive capes, it may only be visible in the crescents or ROIs posterior to the cape. It is difficult to accurately discern flank color in low-quality images or

if a whale carries a heavy diatom load. Young animals tend to have medium flank color, and the flanks of most individuals either darken or lighten as they mature






Example	Category	Description
 MED-ID30412153	Dark	Common in mature individuals and may be exhibited with any cape length. Individuals with this coloration have high contrast between the flank, crescents, and cape.
 MED-ID30605031	Medium	Common in immature individuals, but some adults retain this coloration even after cape differentiation. This coloration will sometimes contain a brown hue.
 MED-ID30509201	Light	Relatively uncommon; the darkest pigmentation on the body is pale gray, with limited contrast against the cape.

Cape pattern

See Table A5.

Table A5 Cuvier's beaked whale capes range from non-existent to being so extensive the individual appears white. Individuals often express different cape patterns at different life stages, especially males. Cape pattern begins at the melon but excludes ovals and

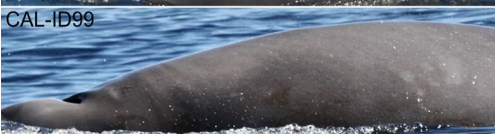
crescents. Without a complete view of the head and post-blowhole regions it can be difficult to accurately score cape pattern, and you may be unable to distinguish between "Discontinuous" and "Variable" patterns

Example	Category	Description
	None	Immature whales that have not started the depigmentation process have no cape pattern.
	Fading	Pale melon transitions to a cape that gradually but continually fades away along its extent, which is usually short.
	Discontinuous	Cape contains depigmented regions that are fully separated by flank color at one or more points along the back starting behind the blowhole and excluding the crescents.
	Variable	Cape is a continuous depigmented region along the body that varies in its shape and brightness throughout its extent and not just at the margins.
	Uniform	Cape is a single, continuous depigmented region that is consistent throughout its extent with the only variations occurring at the margins where the cape fades into the flank.

Cape color

See Table A6.

Table A6 Cape color is the lightest color visible extending from the melon backward. Whales without a photographed melon cannot be scored. If present, cape color can range from gray to white. Diatom coverage and poor lighting can make cape color difficult to accurately score





Example	Category	Description
	None	No cape present. Likely an immature individual and would not be able to be determined from a poor-quality image.
	Gray	Lightest depigmented areas are not white but grayish. This is common in younger animals, but a gray cape may be retained in adults.
	White	Lightest depigmented areas of the body are white.

Cape texture

See Table A7.

Table A7 Cape texture reflects the dominant appearance of the depigmented areas within the cape. Note that the margins of the cape vary in texture for most animals, this score reflects the body of the cape, especially along the top of the back that is visible in most ID images.

Irregular cape textures are often associated with irregular cape patterns. If a cape appears mottled or wavy at the margins but is “Even” along the back, it should be scored as “Even”

Example	Category	Description
MED-ID10505262 	None	Uniformly dark pigment along the entire dorsal surface of the body, no cape.
CAL-ID77 	Wavy	The cape includes irregular bands of pigmentation, typically in a “Discontinuous” or “Variable” pattern throughout its extent.
MED-ID30309301 	Mottled	Patchy, irregular depigmentation within cape, typically in a “Discontinuous” or “Variable” pattern.
CAL-ID150 	Even	Consistent depigmentation throughout the extent of the cape. All “Uniform” patterns are “Even” textured, as are some “Discontinuous” patterns.

Last ROI of cape

See Fig. A2.

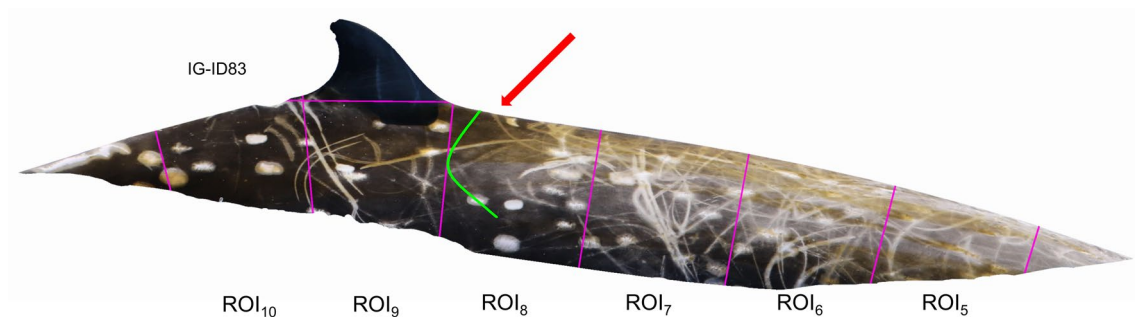


Fig. A2 The last ROI of cape is furthest posterior ROI where depigmentation is present. Immature whales have no cape differentiation (last ROI of cape = 0), individuals just beginning to mature may have depigmentation only on the head (last ROI of cape = 1), and mature whales will have a cape extending beyond ROI₁, sometimes well past

the dorsal fin. In this example, the cape extends to ROI₈, with its posterior margin indicated by a green line. Some capes fade softly into the flank making the end of the cape difficult to determine, especially in individuals with high scarring densities

Supplementary Information The online version contains supplementary material available at <https://doi.org/10.1007/s42991-022-00226-6>.

Acknowledgements We would like to thank the large number of students, interns, volunteers, research staff, and collaborators who have helped collect photos of Cuvier's beaked whales over the years at the three study regions considered here. Data collection in Southern California would not have been possible without the logistical support of many individuals, including our colleagues at MarEcoTel and CRC, including Gregory Schorr, Brenda Rone, Eric Keen and Annie Douglas; our collaborators at the Naval Undersea Warfare Center, including David Moretti, Stephanie Watwood, Ron Morrissey, Susan Jarvis, Nancy DiMarzio, Jessica Ward, and Karin Dolan; the many staff behind the scenes and on the water at the Southern California Offshore Range, and Frank and Jane Falcone. Data collection in the Mediterranean would not have been possible without the support of our colleagues from CIMA Research Foundation including Aurelie Moulins, Paola Tepsich and the CETASMUS interns; and people collecting data during whale watching operations, including Marco Ballardini, Barbara Nani, and Albert Sturlese. We would like to thank the following individuals and organizations for data collection at Guadalupe Island: Andrea Bonilla, Diana Lopez, Jennifer Trickey, Christian Torres, Sergio Martínez, Jay Barlow, Gregory Schorr, Brenda Rone, and volunteers. We also thank the manager of the Biosphere Reserve of Guadalupe Island, Marisol Torres and her team, the local island fishermen, and Mauricio Hoyos for very important logistical support on the island. We also thank Armando Jaramillo, Edwyna Nieto, and Lorenzo Rojas who have supported various key aspects of the projects at Guadalupe. Finally, we thank Eva Hidalgo and crew members of the sailboat Martin Sheen of the Sea Shepherd Conservation Society and of the M/V Storm for their enthusiastic support during the expeditions to Guadalupe.

Author contributions FC: data analysis, data collection, data processing, manuscript preparation. EF: coordination, regional oversight, data collection, data management, manuscript preparation. EK: data collection, data processing, manuscript preparation. GC-H: regional oversight, data collection, manuscript revision. RH-P: data collection, data processing, manuscript revision. MR: regional oversight, data collection, data management, manuscript preparation.

Funding Data collection and processing from California were supported through a series of research grants and contracts awarded to Cascadia Research Collective (2006–2015) and Marine Ecology & Telemetry Research (2016–2019) by the United States Navy's Office of Naval Research, Living Marine Resources Program, and Pacific Fleet Marine Species Monitoring Program. Data collection and processing from Guadalupe Island was supported by grants from the United States Navy Office of Naval Research, Marisla Foundation, International Community Foundation, PADI Foundation, Comisión Nacional de Áreas Naturales Protegidas, Cetacean Society International, and the support of Sea Shepherd Conservation Society. Data collection and analysis from the Mediterranean Sea was partially supported by the Italian "Ministero dell'Ambiente e della Tutela del Territorio e del Mare" (MATTM) and the Pelagos Sanctuary Permanent Secretariat funds.

Availability of data and materials The source data and R code for these analyses are available via dryad: <https://doi.org/10.5061/dryad.bk3j9kddd>.

Declarations

Conflict of interest The authors have no competing interests to declare.

Ethics approval Whales photographed by Marine Ecology & Telemetry Research (MarEcoTel) were primarily approached under scientific research permits 540-1811-04 and 16111 issued to Cascadia Research Collective (CRC) by the US National Marine Fisheries Service, with oversight by the CRC Institutional Animal Care and Use Committee (IACUC). Whales photographed at Guadalupe Island were approached under scientific research permits SGPA/DGVS/09096/16, SGPA/DGVS/02740/17, SGPA/DGVS/000451/18, and SGPA/DGVS/00374/20 issued by Wildlife Department of Secretariat of Environment and Natural Resources of México.

References

- Ackermann MR, Blömer J, Kuntze D, Sohler C (2012) Analysis of agglomerative clustering. *Algorithmica* 69:184–215. <https://doi.org/10.1007/s00453-012-9717-4>
- Baini M, Panti C, Fossi MC, Jiménez B, Coomber FG, Bartolini A, Muñoz-Arnanz J, Moulins A, Rosso M (2020) First assessment of POPs and cytochrome P450 expression in Cuvier's beaked whales (*Ziphius cavirostris*) skin biopsies from the Mediterranean Sea. *Sci Rep* 10(1):1–13. <https://doi.org/10.1038/s41598-020-78962-3>
- Baird RW (2019) Behavior and ecology of not-so-social odontocetes: Cuvier's and Blainville's beaked whales. *Ethology and behavioral ecology of odontocetes. Ethology and behavioral ecology of marine mammals*. Springer, Cham. https://doi.org/10.1007/978-3-030-16663-2_14
- Baird R, Stacey PJ (1988) Variations in saddle patch pigmentation in populations of killer whales (*Orcinus orca*) from British Columbia, Alaska, and Washington State. *Can J Zool* 66:2582–2585. <https://doi.org/10.1139/z88-380>
- Barlow J, Ferguson M, Perrin WF, Ballance L, Gerrodette T, Joyce G, MacLeod CD, Mullin K, Palka D, Waring G (2006) Abundance and density of beaked and bottlenose whales (family Ziphiidae). *J Cetac Res Manage* 7:263–270
- Best PB, Photopoulou T (2016) Identifying the “demon whale-biter”: Patterns of scarring on large whales attributed to a cookie-cutter shark *Isistius* sp. *PLoS ONE* 11:e0152643. <https://doi.org/10.1371/journal.pone.0152643>
- Booth CG, Sinclair RR, Harwood J (2020) Methods for monitoring for the population consequences of disturbance in marine mammals: a review. *Front Marine Sci* 7:115. <https://doi.org/10.3389/fmars.2020.00115>
- Brown AM, Bejder L, Parra GJ, Cagnazzi D, Hunt T, Smith JL, Allen SJ (2016) Sexual dimorphism and geographic variation in dorsal fin features of Australian humpback dolphins, *Sousa sahulensis*. *Adv Mar Biol* 73:273–314. <https://doi.org/10.1016/bs.amb.2015.08.002>
- Cárdenas-Hinojosa G, Hoyos-Padilla M, Rojas-Bracho L (2015) Occurrence of Cuvier's beaked whales (*Ziphius cavirostris*) at Guadalupe Island, Mexico, from 2006 to 2009. *Latin Am J Aquat Mammals* 10:38–47. <https://doi.org/10.5597/lajam00192>
- Caspar KR, Begall S (2022) Sexual dimorphism in toothed whales (Odontoceti) follows Rensch's rule. *Mamm Biol* 102. <https://doi.org/10.1007/s42991-022-00239-1>
- Chen B, Jefferson TA, Wang L, Gao H, Zhang H, Zhou Y, Xu X, Yang G (2018) Geographic variation in pigmentation patterns of Indo-Pacific humpback dolphins (*Sousa chinensis*) in Chinese waters. *J Mammal* 99:915–922. <https://doi.org/10.1093/jmammal/gyy068>
- Civil AM, Cheney B, Quick NJ, Islas-Villanueva V, Graves JA, Janik VM, Thompson PM, Hammond PS (2018) Variations in age- and sex-specific survival rates help explain population trend in a discrete marine mammal population. *Ecol Evol* 9(1):533–544. <https://doi.org/10.1002/ece3.4772>

- Claridge DE (2013) Population ecology of Blainville's beaked whales (*Mesoplodon densirostris*) (Doctoral dissertation, University of St Andrews). <http://hdl.handle.net/10023/3741>. Accessed 23 Feb 2022
- Clutton-Brock T, Sheldon BC (2010) Individuals and populations: the role of long-term, individual-based studies of animals in ecology and evolutionary biology. *Trends Ecol Evol* 25(10):562–573. <https://doi.org/10.1016/j.tree.2010.08.002>
- Coomber FG, Moulins A, Tepsich P, Rosso M (2016a) Sexing free-ranging adult Cuvier's beaked whales (*Ziphius cavirostris*) using natural marking thresholds and pigmentation patterns. *J Mammal* 97:879–890. <https://doi.org/10.1093/jmammal/gyw033>
- Coomber FG, D'Incà M, Rosso M, Tepsich P, Notarbartolo Di Sciarra G, Mullins A (2016b) Description of the vessel traffic within the north Pelagos Sanctuary: inputs for marine spatial planning and management implications within an existing international marine protected area. *Mar Policy* 69:102–113. <https://doi.org/10.1016/j.marpol.2016.04.013>
- Cox TM, Ragen TJ, Read AJ, Vos E, Baird RW, Balcomb K, Barlow J, Caldwell J, Cranford T, Crum L, D'Amico A, D'Spain G, Fernández A, Finneran J, Gentry R, Gerh W, Gulland F, Hildebrand J, Houser D, Hullar T, Jepsen PD, Ketten D, MacLeod CD, Miller P, Moore S, Mountain DC, Palka D, Ponganis P, Rommel S, Rowles T, Taylor B, Tyack P, Wartzok D, Gisiner R, Mead J, Benner L (2006) Understanding the impacts of anthropogenic sound on beaked whales. *J Cetac Res Manage* 7:177–187
- Curtis KA, Falcone EA, Schorr GS, Moore JE, Moretti DJ, Barlow J, Keene E (2020) Abundance, survival, and annual rate of change of Cuvier's beaked whales (*Ziphius cavirostris*) on a Navy sonar range. *Marine Mammal Sci* 37(2):399–419. <https://doi.org/10.1111/mms.12747>
- Dalebout ML, Robertson KM, Frantzis A, EngelHaupt D, Mignucci-Giannoni A, Rosario-Delestre RJ, Baker S (2005) Worldwide structure of mtDNA diversity among Cuvier's beaked whales (*Ziphius cavirostris*): implications for threatened populations. *Mol Ecol* 14:3353–3371. <https://doi.org/10.1111/j.1365-294x.2005.02676.x>
- Falcone EA, Schorr GS, Douglas AB, Calambokidis J, Henderson E, McKenna MF, Hildebrand J, Moretti D (2009) Sighting characteristics and photo-identification of Cuvier's beaked whales (*Ziphius cavirostris*) near San Clemente Island, California: a key area for beaked whales and the military? *Mar Biol* 156:2631–2640. <https://doi.org/10.1007/s00227-009-1289-8>
- Falcone EA, Schorr GS, Watwood SL, DeRuiter SL, Zerbini AN, Andrews RD, Morrissey RP, Moretti DJ (2017) Diving behaviour of Cuvier's beaked whales exposed to two types of military sonar. *R Soc Open Sci* 4(8):170629. <https://doi.org/10.1098/rsos.170629>
- Feyrer LJ, Stewart M, Yeung J, Soulier C, Whitehead H (2021) Origin and persistence of markings in a long-term photo-identification dataset reveal the threat of entanglement for endangered northern bottlenose whales (*Hyperoodon ampullatus*). *Front Mar Sci* 8:349. <https://doi.org/10.3389/fmars.2021.620804>
- Fox J (2016) Applied regression analysis and generalized linear models. Sage, New York
- Gower JC (1971) A general coefficient of similarity and some of its properties. *Biometrics* 27:857–871. <https://doi.org/10.2307/2528823>
- Heyning JE (1989) Cuvier's beaked whale *Ziphius cavirostris* G. Cuvier 1823. In: Ridgway SH, Harrison RS (eds) Handbook of marine mammals. Academic Press, London, pp 289–308
- Hollander M, Wolfe DA, Chicken E (2013) Nonparametric statistical methods, vol 751. Wiley, New York
- Hooker SK, Baird RW, Fahlan A (2009) Could beaked whales get the bends?: effect of diving behaviour and physiology on modelled gas exchange for three species: *Ziphius cavirostris*, *Mesoplodon densirostris* and *Hyperoodon ampullatus*. *Respir Physiol Neurobiol* 167(3):235–246. <https://doi.org/10.1016/j.resp.2009.04.023>
- Ijsseldijk LL, ten Doeschate MTI, Brownlow A, Davison NJ, Deaville R, Galatius A, Gilles A, Haelters J, Jepsen PD, Keijl GO, Kinze CC, Olsen MT, Siebert U, Thøstesen CB, Van Den Broek J, Grøne A, Heesterbeek H (2020) Spatiotemporal mortality and demographic trends in a small cetacean: strandings to inform conservation management. *Biol Cons* 249:108733. <https://doi.org/10.1016/j.biocon.2020.108733>
- Karczmarski L, Chan SCY, Chui SYS, Cameron EZ (2022) Individual identification and photographic techniques in mammalian ecological and behavioural research – Part 2: Field studies and applications. *Mamm Biol (Special Issue)* 102(4). <https://link.springer.com/journal/42991/volumes-and-issues/102-4>
- Kaufman L, Rousseeuw PJ (1990) Finding groups in data: an introduction to cluster analysis. Wiley, New York. <https://doi.org/10.1002/9780470316801>
- Knowlton AR, Kraus SD, Kenney RD (1994) Reproduction in North Atlantic right whales (*Eubalaena glacialis*). *Can J Zool* 72(7):1297–1305. <https://doi.org/10.1139/z94-173>
- Lee HH, Wallen MM, Krzyszczyk E, Mann J (2019) Every scar has a story: age and sex-specific conflict rates in wild bottlenose dolphins. *Behav Ecol Sociobiol* 73(63):1–11. <https://doi.org/10.1007/s00265-019-2674-z>
- MacLeod CD, D'Amico A (2006) A review of beaked whale behaviour and ecology in relation to assessing and mitigating impacts of anthropogenic noise. *J Cetac Res Manage* 7:211–221
- Maechler M, Rousseeuw P, Struyf A, Hubert M, Hornik K (2021) Cluster analysis basics and extensions. R package version 2.1.1. ed.
- Mariani M, Miragliuolo A, Mussi B, Russo GF, Ardizzone G, Pace DS (2016) Analysis of the natural markings of Risso's dolphins (*Grampus griseus*) in the central Mediterranean Sea. *J Mammal* 97:1512–1524. <https://doi.org/10.1093/jmammal/gyw109>
- Martin AR, Da Silva VMF (2006) Sexual dimorphism and body scarring in the Boto (Amazon river dolphin) *Inia Geoffrensis*. *Mar Mamm Sci* 22(1):25–33. <https://doi.org/10.1111/j.1748-7692.2006.00003.x>
- McSweeney DJ, Baird RW, Mahaffy SD (2007) Site fidelity, associations, and movements of Cuvier's (*Ziphius cavirostris*) and Blainville's (*Mesoplodon densirostris*) beaked whales off the island of Hawai'i. *Mar Mamm Sci* 23:666–687. <https://doi.org/10.1111/j.1748-7692.2007.00135.x>
- Mesnick S (2018) Ralls K (2018) Sexual Dimorphism. In: Würsig B, Thewissen JGM, Kovacs KKM (eds) Encyclopedia of marine mammals, 3rd edn. Academic Press, London, pp 848–853
- Moore M, Steiner L, Jann B (2003) Cetacean surveys in the Cape Verde Islands and the use of cookiecutter shark bite lesions as a population marker for fin whales. *Aquat Mamm* 29(3):383–389
- Nelder JA, Wedderburn RWM (1972) Generalized linear models. *J R Stat Soc A* 135:370–384. <https://doi.org/10.2307/2344614>
- New LF, Moretti DJ, Hooker SK, Costa DP, Simmons SE (2013) Using energetic models to investigate the survival and reproduction of beaked whales (family Ziphiidae). *PLoS ONE* 8(7):e68725. <https://doi.org/10.1371/journal.pone.0068725>
- Notarbartolo Di Sciarra G, Agardy T, Hyrenbach DK, Scovazzi T, Van Klaveren P (2008) The Pelagos Sanctuary for Mediterranean marine mammals. *Aquat Conserv Mar Freshwat Ecosyst* 17:367–391. <https://doi.org/10.1002/aqc.855>
- Orbach DN, Packard JM, Piwetz S, Würsig B (2015) Sex-specific variation in conspecific-acquired marking prevalence among dusky dolphins (*Lagenorhynchus obscurus*). *Can J Zool* 93(5):383–390. <https://doi.org/10.1139/cjz-2014-0302>
- Perrin WF (1972) Color patterns of spinner porpoises (*Stenella CF. S. longirostris*) of the Eastern Pacific and Hawaii, with comments on delphinid pigmentation. *Fish Bull* 70:983–1003

- Perrin WF, Reilly SB (1984) Reproductive parameters of dolphins and small whales of the family Delphinidae. Rep Int Whaling Commission Spec Issue 6:97–133
- Pinheiro JC, Bates DM (2000) Mixed-Effects models in S and S-plus. Springer, New York. <https://doi.org/10.1007/978-1-4419-0318-1>
- Pirotta E, Booth CG, Costa DP, Fleishman E, Kraus SD, Lusseau D, Moretti D, New LF, Schick RS, Schwarz LK, Simmons SE, Thomas L, Tyack PL, Weise MJ, Wells RS, Harwood J (2018) Understanding the population consequences of disturbance. Ecol Evol 8(19):9934–9946. <https://doi.org/10.1002/ece3.4458>
- R Core Team (2020) R: a language and environment for statistical computing. R Foundation for statistical computing, Vienna, Austria. <https://www.R-project.org/>. Accessed 23 Feb 2022
- Rasband WS (2011) ImageJ, US National Institutes of Health, Bethesda, Maryland, USA. <http://imagej.nih.gov/ij/>. Accessed 15 Oct 2016
- Robin X, Turck N, Hainard A, Tiberti N, Lisacek F, Sanchez JC, Müller M (2011) pROC: an open-source package for R and S+ to analyze and compare ROC curves. Bioinformatics 12:1–8. <https://doi.org/10.1186/1471-2105-12-77>
- Rosenbaum HC, Clapman PJ, Allen J, Nicole-Jenner M, Jenner K, Florez-González L, Urbán JR, Ladrón PG, Mori K, Yamaguchi M, Baker CS (1995) Geographic variation in ventral fluke pigmentation of humpback whales *Megaptera novaeangliae* populations worldwide. Mar Ecol Prog Ser 124:1–7. <https://doi.org/10.3354/meps124001>
- Rosso M, Ballardini M, Moulins A, Würtz M (2011) Natural markings of Cuvier's beaked whale *Ziphius cavirostris* in the Mediterranean Sea. Afr J Mar Sci 33:45–57. <https://doi.org/10.2989/1814232X.2011.572336>
- Rousseeuw PJ (1986) Silhouettes: a graphical aid to the interpretation and validation of cluster analysis. J Comput Appl Math 20:53–65. [https://doi.org/10.1016/0377-0427\(87\)90125-7](https://doi.org/10.1016/0377-0427(87)90125-7)
- Rowe LE, Dawson SM (2009) Determining the sex of bottlenose dolphins from Doubtful Sound using dorsal in photographs. Mar Mamm Sci 25:19–34. <https://doi.org/10.1111/j.1748-7692.2008.00235.x>
- Royston JP (1982) The W test for normality. J R Stat Soc 31:176–180. <https://doi.org/10.2307/2347986>
- Sakamoto Y, Ishiguro M, Kitagawa G (1986) Akaike information criterion statistics. D. Reidel Publishing Company, Dordrecht
- Schorr GS, Falcone EA, Moretti DJ, Andrews RD (2014) First long-term behavioral records from Cuvier's Beaked Whales (*Ziphius cavirostris*) reveal record-breaking dives. PLoS ONE 9(3):e92633. <https://doi.org/10.1371/journal.pone.0092633>
- Sharma S, Batra N (2019) Comparative study of single linkage, complete linkage, and Ward method agglomerative clustering. In: International Conference on Machine Learning, Big Data, Cloud and Parallel Computing (Com-IT-Con). India. <https://doi.org/10.1109/comitcon.2019.8862232>
- Shaw CN, Wilson PJ, White BN (2003) Methods for gender determination for mammals. J Mammal 20(1):123–128. [https://doi.org/10.1644/1545-1542\(2003\)084%3c0123:ARMMOG%3e2.0.CO;2](https://doi.org/10.1644/1545-1542(2003)084%3c0123:ARMMOG%3e2.0.CO;2)
- Struyf A, Hubert M, Rousseeuw P (1996) Integrating robust clustering techniques in S-PLUS. Comput Stat Data Anal 26:17–37. [https://doi.org/10.1016/s0167-9473\(97\)00020-0](https://doi.org/10.1016/s0167-9473(97)00020-0)
- Tyack PL, Johnson M, Soto NA, Sturlese A, Madsen PT (2006) Extreme diving of beaked whales. J Exp Biol 209(21):4238–4253. <https://doi.org/10.1242/jeb.02505>
- Weiss MN, Franks DW, Giles DA, Youngstrom S, Wasser SK, Balcomb KC, Ellifrit DK, Domenici P, Cant MA, Ellis S, Nielsen MLK, Grimes C, Croft DP (2021) Age and sex influence social interactions, but not associations, within a killer whale pod. Proc R Soc B. <https://doi.org/10.1098/rspb.2021.0617>
- Wickman L, Rayment W, Slooten E, Dawson SM (2021) An observed decline in the mark rate of Hector's dolphins at Banks Peninsula. N Zeal Marine Mamm Sci. <https://doi.org/10.1111/mms.12826>
- Wright AJ, Soto NA, Baldwin AL, Bateson M, Beale CM, Clark C, Deak T, Edwards EF, Fernández A, Godinho A Hatch LT, Kakuschke A, Lusseau D, Martineau D, Romero LM, Weigart LS, Wintle BA, Notarbartolo Di Sciarra G, Martin V (2007) Do marine mammals experience stress related to anthropogenic noise? Int J Comp Psychol 20(2):274–316

Publisher's Note Springer Nature remains neutral with regard to jurisdictional claims in published maps and institutional affiliations.

Springer Nature or its licensor holds exclusive rights to this article under a publishing agreement with the author(s) or other rightsholder(s); author self-archiving of the accepted manuscript version of this article is solely governed by the terms of such publishing agreement and applicable law.